Neutron and Proton Spectra from Targets Bombarded by 160-MeV Protons*

J. W. WACHTER, W. R. BURRUS, AND W. A. GIBSON
Oak Ridge National Laboratory, Oak Ridge, Tennessee
(Received 6 March 1967)

Secondary-neutron spectral data in the energy range between 50 and 160 MeV from targets bombarded by 160-MeV protons have been measured using a proton-recoil spectrometer. Secondary-proton measurements were also made using this spectrometer. The target materials were water, deuterium, beryllium, carbon, aluminum, copper, cobalt, and bismuth; and measurements were made at 0, 10, 45, 60, and 135 deg. Target thicknesses ranged from thin targets in which the primary beam lost only a small amount of energy to thick targets in which the primary beam was completely stopped. The thin-target measurements are expressed as cross sections, and the remainder of the results are expressed as yields. Energy resolutions of 25 and 15% are associated with the neutron and proton spectra, respectively. The results are compared with theoretical results obtained from Monte Carlo nuclear-cascade codes.

I. INTRODUCTION

THIS experiment is one of a series[1,2] conducted at the Oak Ridge National Laboratory to measure the energy spectra of secondary neutrons and protons produced in the interaction of monoenergetic protons with a variety of elements for several primary-proton energies. In the measurements reported here, a 160-MeV proton beam bombarded targets of water, deuterium, beryllium, carbon, aluminum, copper, cobalt, and bismuth, and secondary particles were measured utilizing a proton-recoil spectrometer. The target thicknesses ranged from thick targets in which the primary beam was completely stopped to thin targets in which only a small fraction of the beam energy was lost. The neutron measurements with thick targets were made at angles of 0, 10, and 45 deg from the incident beam and the results are expressed as yields, and those with thin targets (cobalt and bismuth only) were made at an angle of 45 deg. The data from the latter measurements are reported as cross sections rather than yields. Thick-target proton measurements were made at angles of 0, 10, 45, and 135 deg, and thin-target measurements were made at 60 and 135 deg.

The experimental apparatus used for the measurements is described briefly in Sec. II, and the experimental techniques are reviewed in Sec. III. Section IV describes the techniques of data analysis which are unique for this type of spectrometer, and Sec. V presents the data in the form of graphs. Finally, Sec. VI compares the results with Monte Carlo calculations and describes the procedures required to prepare the calculated data so that the comparison accounts for the particular geometry and energy resolution of the spectrometer.

Secondary-proton spectra made under similar conditions to those presented here have been reported by Wall and Roos[3] for 160-MeV incident protons and by Dalgren *et al.*[4] for 185-MeV incident protons.

II. SPECTROMETER

The proton-recoil spectrometer used for the measurements is described in detail elsewhere[5] and is shown in Fig. 1. During the proton measurements the radiator and the anticoincidence counter shown in the figure were removed and secondary protons from the target passed through the coincidence counters A, B, and C. Counters A and B were organic scintillators which reduced background counts, and counter C was a thin NaI(Tl) scintillator (1.464g/cm² thick) which when penetrated by a proton produced a light pulse with an average amplitude

$$l \cong \int_0^T (dl/dE)(dE/dx)dx, \qquad (1)$$

where T is the thickness of the scintillator, dE/dx is the mean energy loss per unit path length, and dl/dE is the scintillation efficiency. The resulting pulse-height

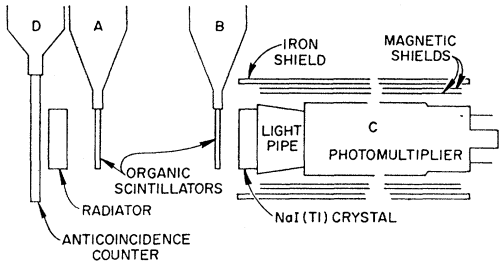

FIG. 1. Proton-recoil spectrometer used to make neutron measurements. The radiator and anticoincidence counter were removed for proton measurements.

*Research sponsored by the National Aeronautics and Space Administration under Union Carbide Corporation's contract with the U. S. Atomic Energy Commission.

[1] R. W. Peelle, T. A. Love, N. W. Hill, and R. T. Santoro, Oak Ridge National Laboratory Report No. ORNL-3887, 1966 (unpublished).

[2] W. Zobel, F. C. Maienschein, and R. J. Scroggs, Oak Ridge National Laboratory Report No. ORNL-3506, 1965 (unpublished).

[3] N. S. Wall and P. R. Roos, Phys. Rev. **150**, 811 (1966).

[4] S. Dahlgren *et al.*, Arkiv Fysik **32**, 510 (1965).

[5] W. A. Gibson, W. R. Burrus, J. W. Wachter, and C. F. Johnson, Nucl. Instr. Methods **46**, 29 (1967).

spectrum was accumulated in a multichannel analyzer. If resolution effects are ignored, Eq. (1) leads to a unique value of proton energy corresponding to each pulse height for protons with less than the minimum ionizing energy.

During the neutron measurements, secondary neutrons from the target interacted with the radiator to produce recoil protons, which passed through counters A, B, and C as described above. In this case the recoil proton energy is related to the secondary neutron energy by

$$E_p = E_n \cos^2\theta/(1+E_n \sin^2\theta/2Mc^2), \quad (2)$$

where θ is the angle between the path of the neutron and the path of the recoiling proton, M is the mass of the nucleons, and E_p and E_n are the energies of the recoil proton and neutron, respectively. Counts due to secondary protons from the target were eliminated by the anticoincidence counter D placed in front of the radiator.

The above equations form the basic relationships between pulse height and energy used in the data analysis; however, a rigorous analysis technique must also consider the ambiguities between energy and pulse height introduced by resolution effects. (The inclusion of these effects in the analysis techniques is described briefly in Sec. IV.)

The resolution of a distribution is defined as

$$R = \frac{\text{full width at half maximum (FWHM) of the distribution}}{\text{centroid of distribution}}. \quad (3)$$

The pulse-height distribution is the distribution obtained by illuminating the spectrometer with a monoenergetic particle beam, and the energy resolution is defined as the resolution of the distribution obtained by transforming the pulse-height distribution with a one-to-one relation between pulse height and energy.

In the neutron measurements the major factors determining the energy resolution were (1) the maximum scattering angle between the neutron and recoil proton as defined by the geometry of the apparatus and the thickness of the radiator; and (2) the Landau spread caused by the energy lost by monoenergetic protons in the $\Delta E/\Delta x$ counter.[6,7] In the proton measurements only the latter effect influenced the resolution. The thickness of the $\Delta E/\Delta x$ counter was chosen, in both sets of measurements, so that the largest resolution due to energy-loss fluctuations was about 20% for the pulse-height spectrum (this occurred at the maximum energy of 160 MeV). The energy resolution is larger than the pulse-height resolution at high energies. The geometry and thickness of the radiator used for the neutron measurements were chosen so that the maximum neutron energy resolution due to the scattering angle and the radiator thickness was 15%.

The data-analysis technique required a determination of the several pulse-height distributions which would result if the spectrometer were illuminated by a series of monoenergetic neutron beams covering the range of energy response of the spectrometer. These distributions are termed the neutron response functions of the spectrometer. Since these functions would be difficult to obtain experimentally, they were calculated by the Monte Carlo techniques described in Refs. 5 and 8. The calculated neutron response functions are shown in Fig. 2 for three different monoenergetic neutron beams, and the corresponding energy distributions are shown in Fig. 3. Figure 4 shows the resolution of these distributions as a function of energy.

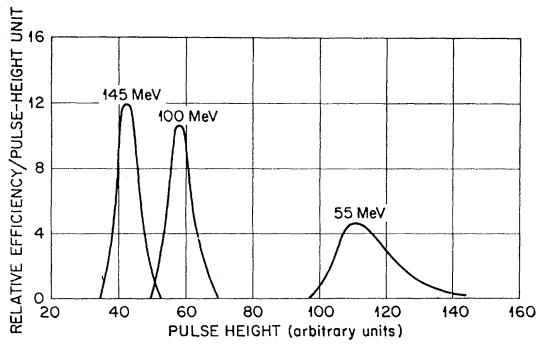

FIG. 2. Relative efficiency per pulse-height unit versus pulse height for three different neutron energies incident on radiator. The distributions were calculated using a Monte Carlo technique and include the major resolution effects.

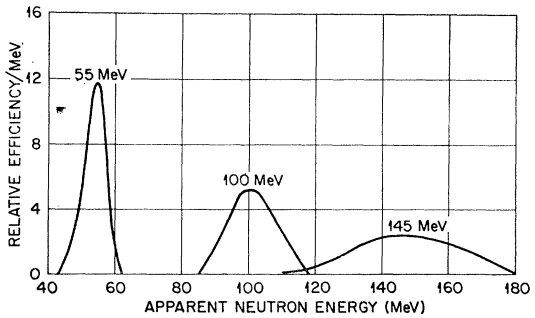

FIG. 3. Apparent neutron energy distributions. These distributions were obtained by transforming the distributions displayed in Fig. 2 with a one-to-one relation between energy and pulse height.

[6] B. Rossi, *High Energy Particles* (Prentice-Hall, Inc., Englewood Cliffs, New Jersey, 1952), p. 22.

[7] D. M. Ritson, in *Techniques of High Energy Physics*, edited by D. M. Ritson (Interscience Publishers, Inc., New York, 1961), p. 18.

[8] W. E. Kinney and J. W. Wachter, Oak Ridge National Laboratory Report No. ORNL-3499, 1963 (unpublished).

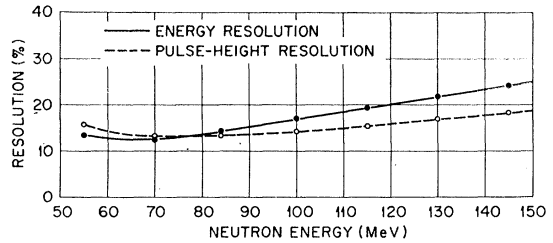

FIG. 4. Calculated pulse-height and energy resolutions of spectrometer as a function of energy. These resolutions are the resolutions of the distributions illustrated in Figs. 2 and 3 as defined in Eq. (3).

Protons resulting from the interaction of neutrons in the carbon of the polyethylene radiator, in the back surface of the anticoincidence counter and in the front surface of counter A, were subtracted by making background measurements using a carbon radiator containing the same areal density of carbon as the polyethylene radiator.

Except for very low-energy recoils, protons with insufficient energy to penetrate counter C produced pulses equal in magnitude to a higher-energy proton of a particular energy which did penetrate the counter. This ambiguity was eliminated by rejecting the lower-energy protons on the basis of a dE/dx determination in counter B.

III. EXPERIMENTAL SETUP

Figure 5 is a diagram of the experimental setup. The 160-MeV proton beam from the Harvard University synchrocyclotron was focused so that it was incident on the target in an area approximately 0.6 cm in diam. A helium-filled ion chamber was used to integrate the total beam on the target and was calibrated using a Faraday cup.[9] The calibration was known to better than 5% and was shown to be constant over a wide range of beam intensities, including the maximum intensity available.

The energy of the proton beam at the target was

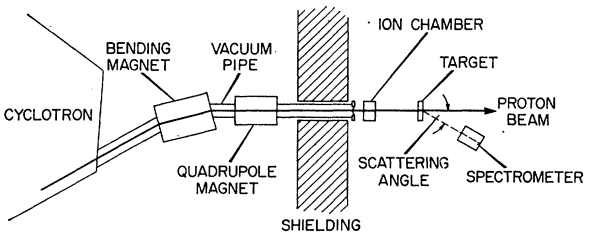

FIG. 5. Experimental setup for making neutron and proton spectral measurements.

[9] R. T. Santoro and R. W. Peelle, Oak Ridge National Laboratory Report No. ORNL-3505, 1964 (unpublished).
[10] M. Rich and R. Madey, University of California Radiation Laboratory Report No. UCRL-2301, 1954 (unpublished).
[11] M. Berger and S. Seltzer, U. S. At. Energy Comm. Natl. Acad. Sci. Natl. Res. Council Publ. 1133, 69 (1964).

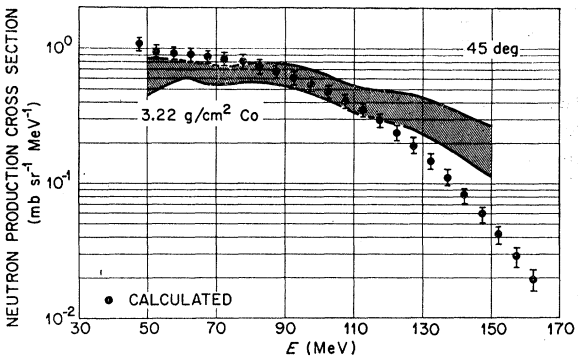

FIG. 6. Experimental and calculated neutron production cross sections as a function of energy at 45 deg for a 3.22-g/cm²-thick cobalt target. The lines enclose the 68% confidence interval and include statistical uncertainties, as well as uncertainties in calculating the efficiency of the spectrometer. The spectrum has a 25% Gaussian energy resolution associated with it. The target thickness was such that the primary beam lost 12 MeV in passing through the target. The theoretical values were calculated from the Monte Carlo intranuclear cascade code and were smeared with a 25% Gaussian energy resolution.

measured several times during the experiment using a range telescope with copper absorbers. The effective range in copper, including the energy loss in the counters, was 26.7±0.1 g/cm², which, using the range tables of Rich and Madey,[10] corresponds to a beam energy at the target of 160.4±0.4 MeV. The multiple-scattering correction[11] was small and was not included in this value.

IV. DATA ANALYSIS

The spectrometer data were recorded in the form of pulse-height distributions from the $\Delta E/\Delta x$ counters.

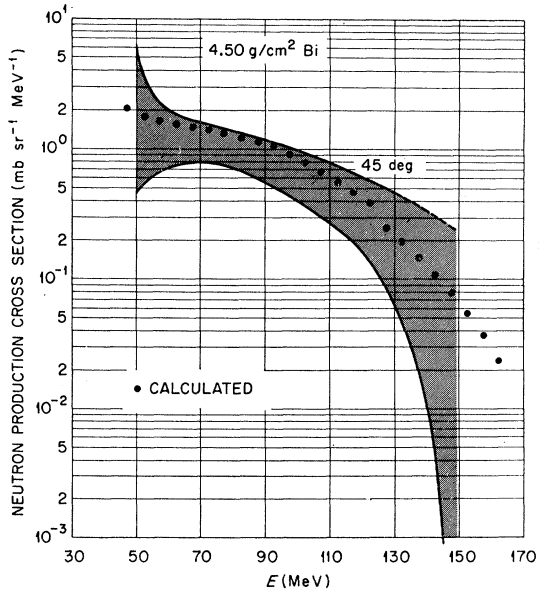

FIG. 7. Experimental and calculated neutron production cross sections at 45 deg from a 4.50-g/cm²-thick bismuth target. The target absorbed 12 MeV from the primary-proton beam.

It is difficult to interpret these measured pulse-height distributions directly because the energy versus mean pulse-height relation is backwards and nonlinear, and the line shapes for monoenergetic radiation are skewed and of variable widths. The detection efficiency for neutrons also changes as a function of neutron energy. Thus we would like to transform the measured pulse-height distributions into estimated spectra which appear to have been obtained directly using an imaginary, or pseudo-, spectrometer having a more desirable line shape, a linear relation between energy and pulse height, and a constant efficiency. In addition to an estimated spectrum, it is necessary, of course, to estimate the errors due to statistical fluctuations in the pulse-height distributions and to uncertainties in the response of the spectrometer.

A generalized technique designed to meet these requirements is the SLOP (simple linear optimization procedure) computer code. This code, the principles of which have been described elsewhere,[12,13] is designed to operate upon experimentally measured pulse-height distributions and to transform them to estimated spectra. In addition to the measured pulse-height distributions, it is necessary to supply the SLOP code with the response of both the actual spectrometer and the pseudospectrometer. The response functions required are the probability distributions that a particle of a particular energy will produce a pulse in a particular channel. In the case of neutrons, the response functions were calculated using a Monte Carlo technique as described in Sec. II. In the case of protons, the response functions for the thick-target data were determined entirely by the Landau energy-loss fluctuations in the $\Delta E/\Delta x$ counter, which, as is pointed out in Sec. II, is the major factor in determining the resolution. For the thin-target data, which were to be expressed in cross sections, it was desirable that the response functions also account for the energy loss of the secondary protons in the target which would otherwise produce a distortion of the spectra. Thus for the thin targets the energy-loss distribution in the target was included in the response functions so that the cross sections are corrected to a "zero-thickness" target. No correction was made for the energy loss of the primary beam, and equal generation of secondaries in all parts of the target was assumed. The response of the pseudospectrometer may be chosen freely by the experimenter subject to certain restrictions which will be discussed.

The output of the SLOP code is an estimated spectrum with a confidence interval which is jointly determined by the statistics of the experimental pulse-height distribution, the error assigned to the response function of the real spectrometer, and the closeness of fit which the code is able to obtain between combinations of the response functions of the real spectrometer and the response functions of the pseudospectrometer. The

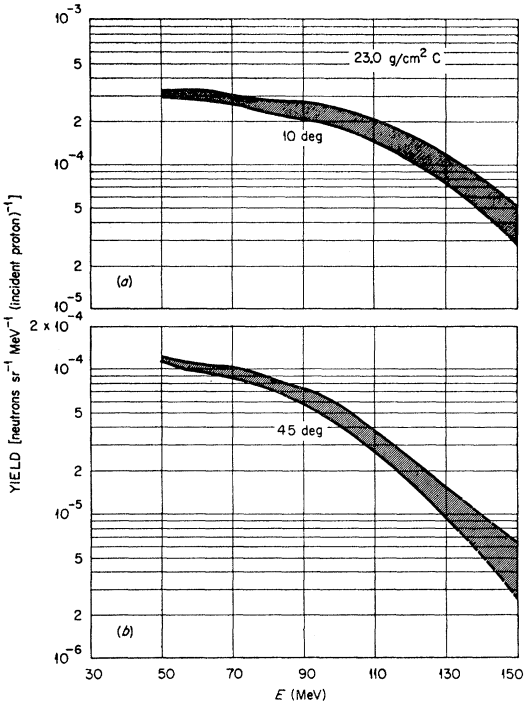

FIG. 9. Experimental neutron yields as a function of energy at 10 and 45 deg from a 23.0-g/cm²-thick carbon target.

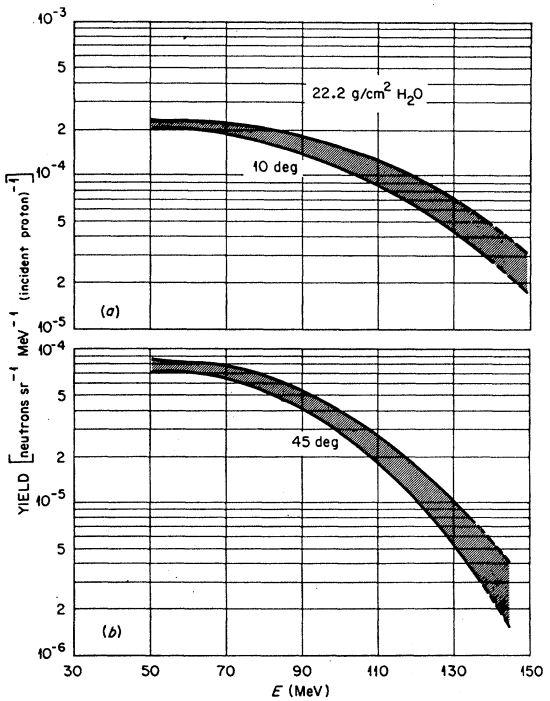

FIG. 8. Experimental neutron yields as a function of energy at 10 and 45 deg from a 22.2-g/cm²-thick water target.

[12] W. R. Burrus and V. V. Verbinski, American Nuclear Society Report No. ANS-SD-2, 1965 (unpublished).
[13] W. R. Burrus, Oak Ridge National Laboratory Report No. ORNL-3743, 1965 (unpublished).

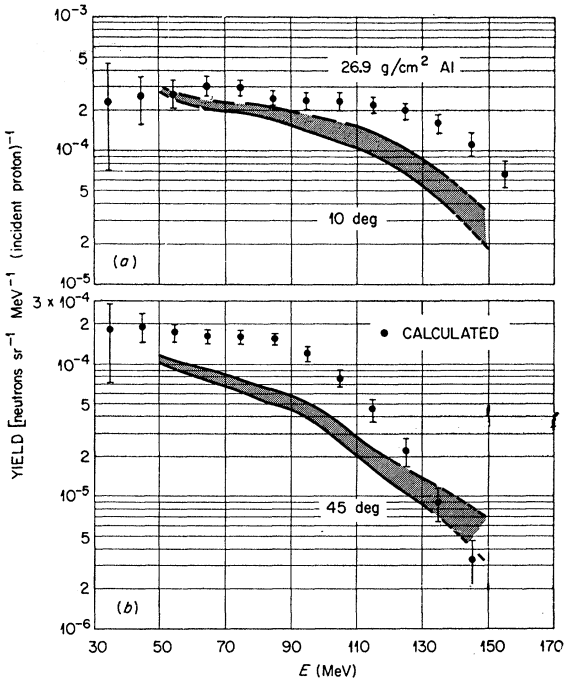

FIG. 10. Experimental and calculated neutron yields as a function of energy at 10 and 45 deg to a 26.9-g/cm²-thick aluminum target. The calculated points were obtained using the Monte Carlo transport codes of Kinney and were smeared using a Gaussian energy resolution with a FWHM of 25%, so that they correspond to the resolution associated with the experimental curves.

results are presented graphically in the form of a cross-hatched band corresponding to the 68% confidence level for each point of the estimated spectrum.

The pseudospectrometer was chosen to have a simple Gaussian energy response (line shape) with a resolution (FWHM) of 25% for neutrons and 15% for protons. The pseudo pulse-height distributions therefore appear as though they were obtained with a spectrometer with a symmetrical Gaussian response. These data are thus in a form suitable for direct comparison with other results measured with the same resolutions (25 or 15%). For comparison with data made with a different resolution, the data with the better resolution may be smeared so that they have comparable resolution.

The pseudospectrometer was not chosen to have a very good energy resolution since a large confidence interval for the resulting estimated spectrum would have been obtained. The resolution employed therefore was chosen to be comparable with that of the actual spectrometer.

The neutron data were taken with three different radiator thicknesses. The thin radiators yielded spectra with the required resolution at low energies but with poor counting statistics at high energies. The thick radiator gave adequate counting statistics at high energies but unacceptable resolution at low energies. The spectra obtained with all three radiator thicknesses were combined in a statistically consistent manner with the SLOP code. Background measurements made with the carbon radiators were subtracted.

TABLE I. Neutron measurements.

Target material	Thickness (g/cm²)	Angle (deg)	Radiator distance[a] (cm)
H_2O	22.2	10	45.2
H_2O	22.2	45	42.5
C	23.0	10	40.1
C	23.0	45	38.3
Al	26.9	10	38.1
Al	26.9	45	36.7
Cu	32.0	10	34.4
Cu	32.0	45	33.8
Co	128	0	32.4
Co[b]	3.22	45	32.4
Bi	44.3	10	35.0
Bi	44.3	45	34.3
Bi[b]	4.50	45	17.4

[a] This distance was used to determine the solid angle subtended by the radiator (see text) and was measured from the point where the incident proton beam line penetrated the assumed neutron birth plane to the front of the radiator. The assumed birth plane for the 128-g/cm²-thick cobalt target and the targets used for the cross-section measurements was the face of the target nearest the spectrometer (back face). For the remainder of the measurements the birth plane was at a distance equal to one-half the range of a 160-MeV proton from the front face of the target.
[b] These measurements are expressed as cross sections.

The efficiency for detecting a neutron is nearly proportional to the solid angle subtended by the radiator as measured from the birth point of the neutron. In order to simplify the calculations of efficiency, all neutrons were assumed to be born at the target face nearest the spectrometer (back face). This assumption

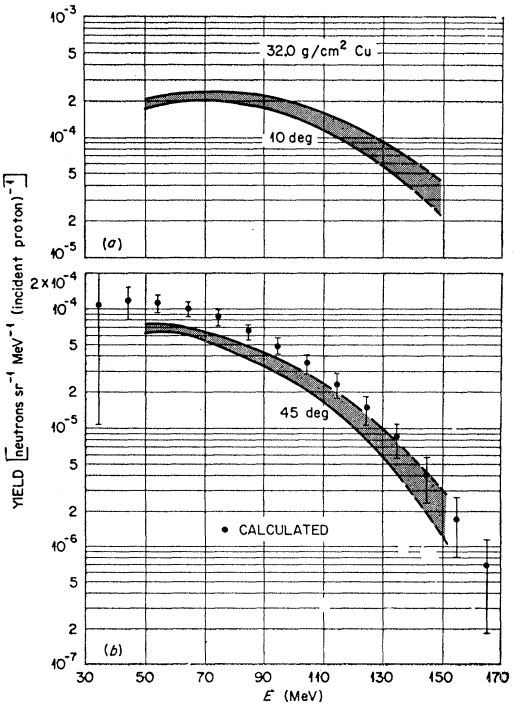

FIG. 11. Experimental and calculated neutron yields at 10 and 45 deg from 32.0-g/cm²-thick copper target.

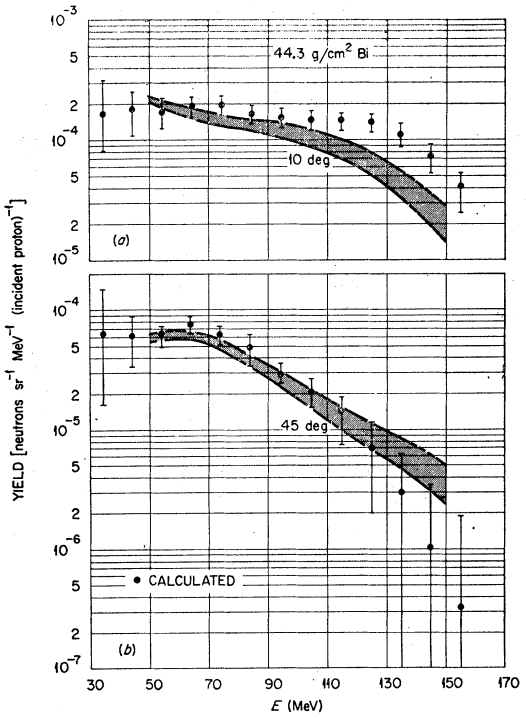

FIG. 12. Experimental and calculated neutron yields at 10 and 45 deg from a 44.3-g/cm²-thick bismuth target.

is sufficient for thin targets; however, for thick targets the neutrons may be born a considerable distance from this plane, resulting in an actual efficiency considerably lower than the calculated efficiency. This is especially true for high-energy neutrons produced by protons that have suffered little slowing down. Thus the neutron spectra presented have been corrected to correspond to a spectrometer efficiency which assumes that the neutrons were born at a distance from the front face equal to one-half of the range of 160-MeV protons. With this choice the maximum deviation in solid angle for aluminum is 23% for neutrons born at the front face and 15% for those born at a distance equivalent to 50 MeV from the end of the 160-MeV proton range.

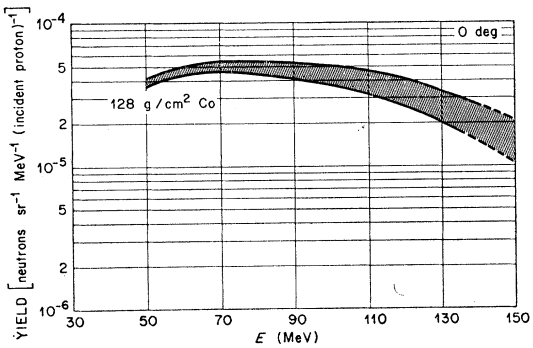

FIG. 13. Experimental neutron yields at 0 deg to the incident beam from a 128-g/cm²-thick cobalt target.

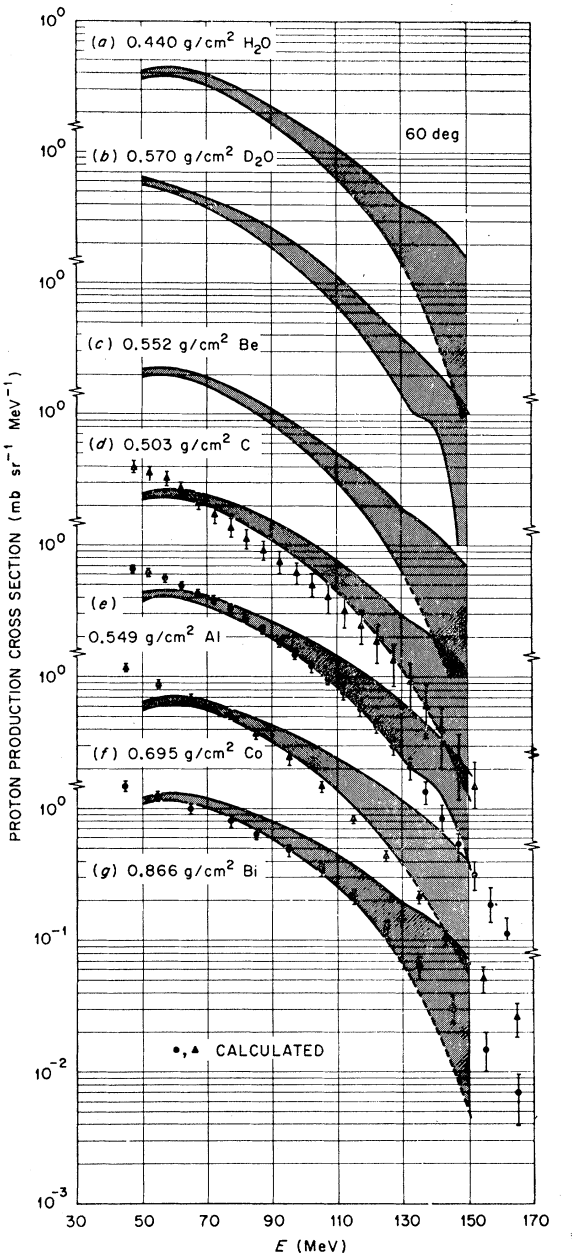

FIG. 14. Experimental and calculated proton cross sections at 60 deg for a variety of elements. The points are the calculated cross sections of Bertini smeared with a 15% Gaussian energy resolution so as to correspond to the energy resolution associated with the experimental results. The targets were at an angle of 30 deg to the incident beam.

The distance from the assumed birth plane to the front of the radiator for each target and angle is listed in Table I. The angle between the beam and the spectrometer was measured at the back face of the target although the actual angle will be somewhat less than this. In the case of the neutron measurements with the thin cobalt and bismuth targets (the cross-section measurements) and with the 128-g/cm² cobalt target, the

TABLE II. Proton measurements.

Material	Angle	Target thickness (g/cm²)	Counter distance[a] (cm)	Spectra[b]
H_2O	10	22.2	46.7	*Y*
	45	22.2	46.7	*Y*
	60	0.44	31.7	*C*
D_2O	60	0.57	31.7	*C*
Be	60	0.552	31.7	*C*
	135	0.552	31.7	*C*
C	60	0.503	31.7	*C*
	45	23.0	46.7	*Y*
	135	0.503	31.7	*C*
	135	5.78	31.7	*Y*
Al	10	26.9	46.7	*Y*
	45	26.9	46.7	*Y*
	60	0.549	31.7	*C*
	135	0.549	31.7	*C*
Cu	0	32.0	46.7	*Y*
	10	32.0	46.7	*Y*
Co	0	128	31.7	*Y*
	45	3.22	46.7	*Y*
	45	7.68	46.7	*Y*
	60	0.695	31.7	*C*
	135	0.695	31.7	*C*
	135	7.68	31.7	*Y*
Bi	10	44.3	46.7	*Y*
	60	0.866	31.7	*C*
	135	0.866	31.7	*C*
	135	4.50	31.7	*Y*
	135	11.3	31.7	*Y*
	135	44.3	31.7	*Y*

[a] This is the distance from the point where the beam line intersects the back of the target to the front of the energy-detecting counter.
[b] *Y* refers to yield expressed in protons/(sr MeV proton) and *C* refers to cross section expressed in mb/(sr MeV).

birth plane was assumed to be the back face of the target.

The efficiency for detecting protons was determined solely by the solid angle subtended by the energy-detecting counter. In all measurements protons were assumed to be born at the point where the incident beam line penetrated the back face of the target, and the distance from this point to the counter is listed in Table II.

The proton spectra were analyzed in a manner similar to that used for the neutron spectra except that no radiators were used and no background corrections were made.

V. DATA

Three groups of neutron measurements were made, differing by the target thicknesses used. In the first group cobalt and bismuth targets were used whose thicknesses, 3.22 and 4.50 g/cm², respectively, were small compared to the nuclear mean free path. Since the incident protons lost only 12 MeV in penetrating these targets, the data are presented as differential cross sections ($d^2\sigma/d\Omega dE$). In the second group of measurements the target thicknesses were sufficiently large to stop the primary protons; however, the probability

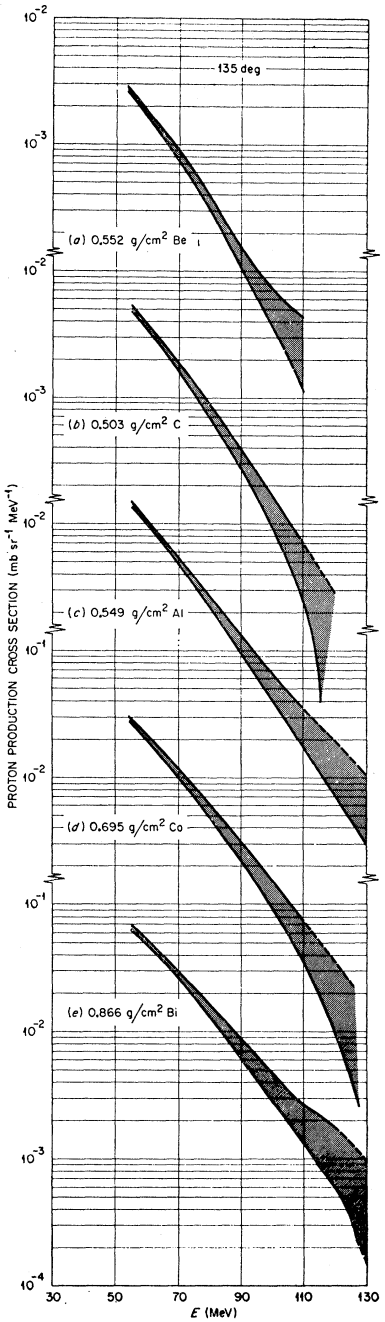

FIG. 15. Proton cross sections at 135 deg to the incident beam for a range of elements. No significant difference in the spectral shape is evident between various elements; however, the systematic increase of the cross section with atomic weight is noted. It was necessary to cut off the spectra well below the primary beam energy due to the interference from gamma rays discussed in the text.

of a secondary particle undergoing an interaction within the target was small (<30%). The third group was the measurement of the neutron spectra at 0 deg from a 128-g/cm²-thick target. In this case the probability for the secondaries undergoing interactions within the

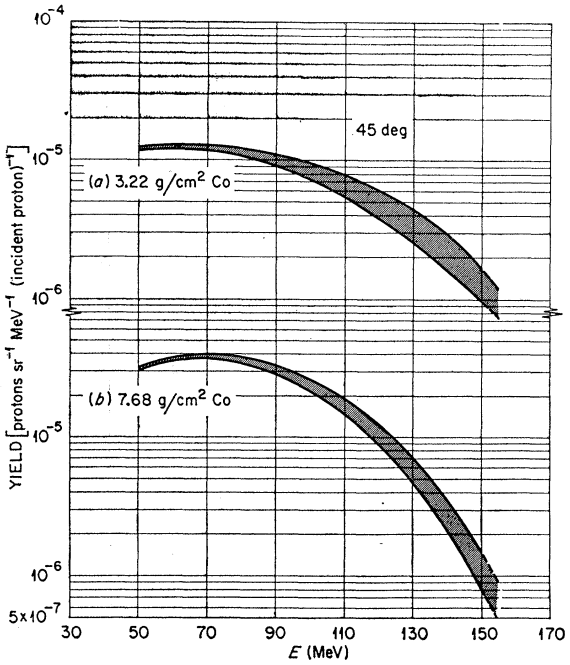

FIG. 16. Proton yield at 45 deg from cobalt targets which absorbed 12 and 28 MeV from the primary-proton beam.

target was large, and these results represent an example of a true nucleon transport. The results from the second and third groups of measurements are presented as differential yields.

The proton measurements were made for similar groups of target thicknesses, and since the efficiency of the spectrometer for detecting protons was much larger, more cases were studied and the statistical errors are much smaller. Differential cross-section data were made at 60 and 135 deg using thin targets. Yield measurements were made at 0, 10, 45, and 135 deg using targets which either absorbed a large fraction of the energy from the primary-proton beam or were thicker than the range of the primary protons. It is noted that in the latter case the emerging protons at forward angles must be a result of secondary neutrons interacting and producing protons sufficiently close to the surface of the target to escape.

Table I lists the elements, target thicknesses, and angles at which measurements were made for neutrons, and Table II lists the data for protons. Some of the spectra have been reported previously[5,14]; however, improvements have been made in the analysis code and the results presented below supersede the previous ones. Figures 6–13 give the neutron data, and Figs. 14–21 give the proton data.

A large number of gamma rays were produced by the interaction of the protons in the target. Some of these gamma rays interacted in the target, as well as in the radiator and counters of the spectrometer, and produced electrons which were counted in the spectrometer and produced pulses that had the same heights as those produced by high-energy protons. These events produced a rapid rise of the spectra in the analyzed data at high energies and were especially troublesome for the proton measurements at back angles where the proton cross section was small. For neutron measurements background subtractions were made and the effect of electron counts was nearly eliminated. The portions of the spectra with significant

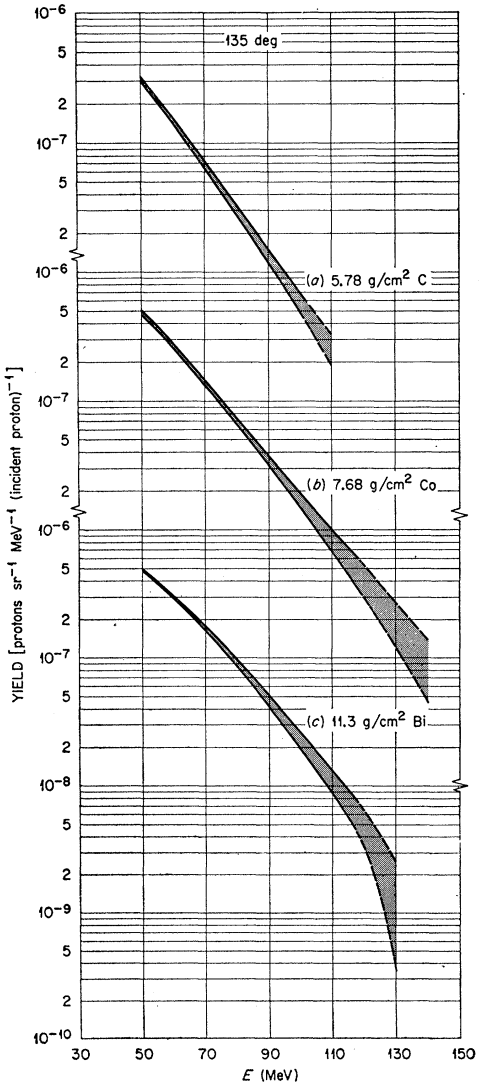

FIG. 17. Proton yields at 135 deg for several elements. The target thicknesses were chosen so that the primary protons lost about 28 MeV in traversing the target.

[14] W. A. Gibson, W. R. Burrus, W. E. Kinney, J. W. Wachter, and C. F. Johnson, in *Second Symposium of Protection Against Radiations in Space*, edited by Arthur Reetz, Jr. (National Aeronautics and Space Administration, Washington, D. C., 1965), p. 337.

contributions from the electrons have been omitted from the results presented here, and the dashed portions of the curves are extrapolations of the nucleon spectra into regions where contributions from the electrons were apparent.

VI. COMPARISONS WITH MONTE CARLO CALCULATIONS

One of the major reasons for conducting these measurements was to provide cross-section and nucleon transport data to compare with the theoretical Monte Carlo nuclear cascade calculations being made by Bertini[15] and Kinney[16] at Oak Ridge National Laboratory and elsewhere. In the Bertini calculations the nucleons were assumed to move independently in a nucleus that had a three-region nucleon density distribution approximating the distribution found by

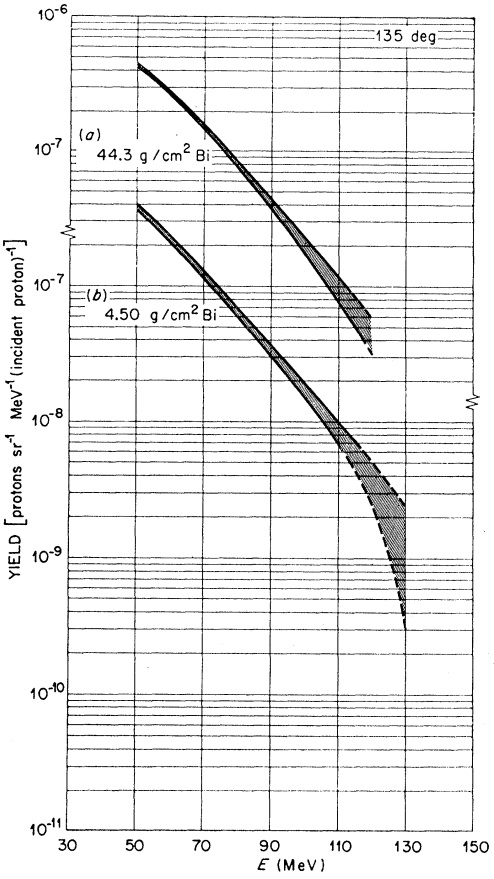

FIG. 18. Proton yields at 135 deg to the incident beam from bismuth targets of different thicknesses. The similarity between the yield spectra results from the fact that back-scattered protons are of low energy and must be born near the surface to escape; thus only protons from a thin layer of the target contribute to the yield.

[15] H. W. Bertini, Phys. Rev. **131**, 1801 (1963); **138**, AB2 (1965).
[16] W. E. Kinney, Oak Ridge National Laboratory Report No. ORNL-3610, 1964 (unpublished).

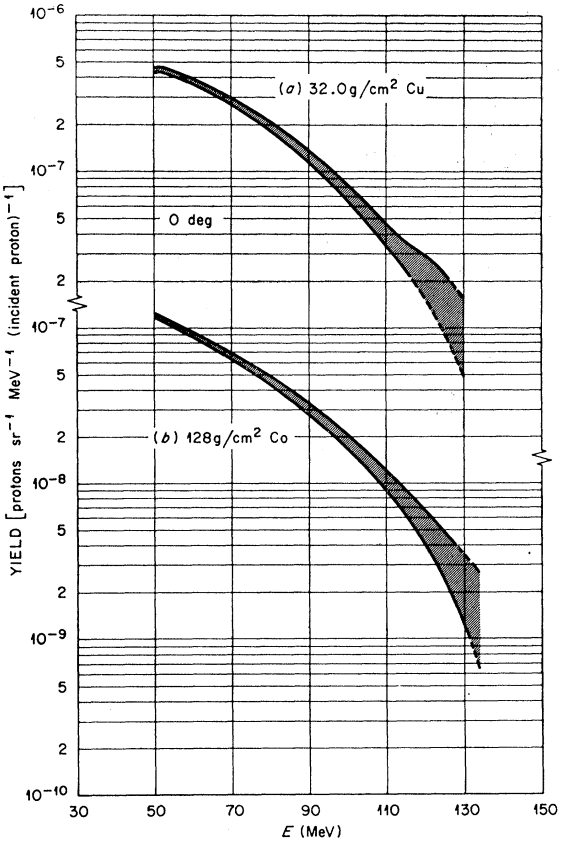

FIG. 19. Proton yields at 0 deg from thick copper and cobalt targets.

electron scattering. Table III lists the radii of the three regions for the elements considered in the present comparisons. The nucleons were assumed to have a zero-temperature Fermi momentum distribution in each region. The interaction of the incident nucleon and the nucleons in the nucleus was considered to be a free-particle interaction. Using this model and the free-particle interaction cross sections, the Monte Carlo program calculated the energy spectrum and angular distribution of particles emerging from the struck nucleus. The code also included an evaporation calculation; however, no contribution to the neutron production above 50 MeV is predicted to result from evaporation.

A major justification for describing the interaction

TABLE III. Outer radii of nuclear regions used in nuclear model.

Element	Central region (F)	Middle region (F)	Outer region (F)
C	1.31	3.22	4.96
Al	2.03	3.97	5.72
Co	2.97	4.93	6.68
Cu	3.11	5.06	6.81
Bi	5.16	7.11	8.86

between the incident and target nucleons by classical kinematics involving only pairs of nucleons is that λ, the DeBroglie wavelength divided by 2π, of the incident particle is much smaller than the mean free path within the nucleus. To investigate the validity of this assumption consider the case of bismuth where the model's central nucleon density is the greatest and the core regions are the largest of the nuclei considered. Protons incident on the nucleus present the most severe test of the model due to the neutron excess and the relative larger n-p cross section over the p-p or n-n. An energy of 50 MeV is the lowest considered, and for thick targets secondary or degraded protons of this energy are possible.

Due to the potential well an incident 50-MeV proton will have a kinetic energy of about 90 MeV in the central core region with a λ of 0.52 F. In the central core region

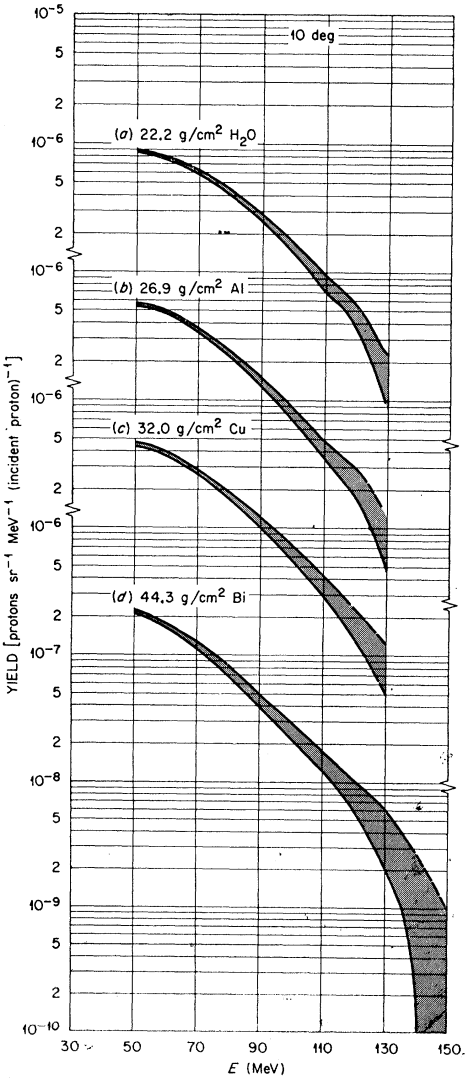

FIG. 20. Thick-target proton yields at 10 deg for a variety of elements.

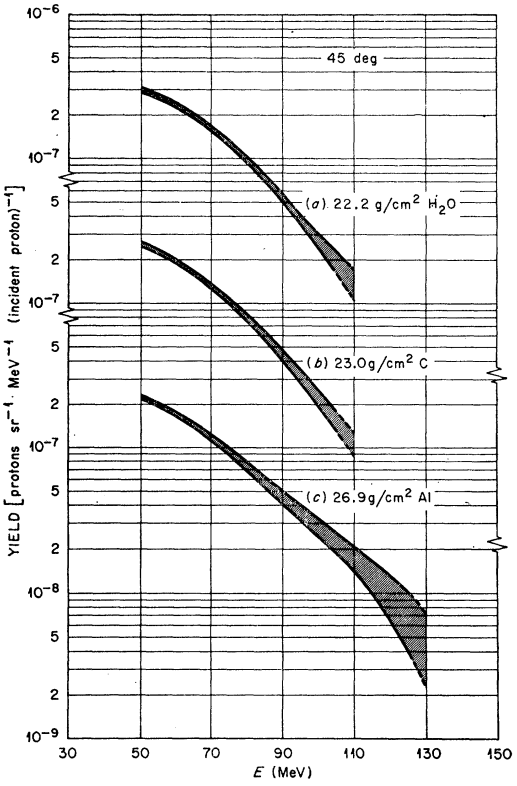

FIG. 21. Thick-target proton yields at 45 deg from water, carbon, and aluminum targets.

the nucleon density is 1.77×10^{38}/cm³ and using the cross sections used in the calculation this leads to a mean free path of 0.88 F. The exclusion principle decreases the probability for interaction[17] and results in an effective mean free path of about 1.1 F and the ratio of the mean free path to λ is 2.2. The ratio of the mean free path to λ will be larger in the outer regions of the nucleus as well as in lighter nuclei. A detailed calculation would take into account the relative motion of the target nucleons in the nucleus; however, these effects will be ignored here. In most of the calculations presented here the worst cases are far too restrictive; e.g., the ratio of the mean free path to λ in the central core for a 160-MeV proton incident on bismuth is approximately 5.4. In summary the ratio of the mean free path to λ for the worst case example varies from 2.2 at 50 MeV to 5.4 at 160-MeV incident energy. Noting the shortcomings of this type of plausibility argument a reasonable conclusion appears to be that at the lowest energy considered here the model is marginal but may give adequate results. At the highest energies, the model appears to be well justified. However, because of the many assumptions incorporated into the model, detailed justification must depend upon comparison with experiment.

[17] M. L. Goldberger, Phys. Rev. 74, 1269 (1948).

In the case of thick targets a code written by Kinney transported the secondary nucleons emerging from the struck nucleus through the target by further application of Monte Carlo techniques.

Comparisons between the calculations of Bertini and Kinney and the measurements are presented here for neutrons and protons from thin targets and for neutrons from thick targets. No comparisons were made for protons from thick targets or for protons emerging at 135 deg, since the probability for proton emission is so small that with the present Monte Carlo program no significant data could be obtained from the code in a reasonable amount of computer time.

In order to make meaningful comparisons the following conditions must be met:

(1) The solid angles considered must be nearly the same for the calculations and experiments. Since the angular resolution of the spectrometer was between 5 and 10 deg for neutrons and was somewhat smaller for protons, bin widths of 5 deg were chosen for the Monte Carlo calculation.

(2) The energy resolution must be the same for the calculation and experiment. Since the theoretical results assume precise energies which were grouped in bins 5 MeV wide, the calculated results were smeared with the experimental resolution. The experimental resolution was Gaussian with a resolution of 25% for neutrons and 15% for protons.

(3) In the case of the thick neutron targets, the beam spreads considerably as it passes through the target and the interaction takes place at various depths. Thus the dispersion in angles impinging on the radiator of the spectrometer is increased. The Monte Carlo calculation for neutrons produced in thick targets was modified so that all neutrons were counted if they impinged on the area corresponding to the radiator in the experiment. The assumed birth plane in the calculation was chosen to correspond to the birth plane chosen for the measurements. Thus the geometry in the calculation accurately reproduced the experimental geometry.

The calculated results are plotted along with the experimental results on Figs. 6, 7, 10, 11, 12, and 14. The errors associated with the calculated points are the statistical errors of the Monte Carlo calculation. In general the agreement between the experimental and theoretical results is quite good and justifies the basic model used in the Monte Carlo calculations. There is no significant disagreement between the experimental results presented here and the cross-section calculations; however, there is disagreement for thick-target comparisons. In particular, at 45 deg, the calculation lies considerably above the experimental results at low energies, especially for aluminum. The agreement becomes better for the heavier elements. At 10 deg, disagreement appears at high energies where the results of the calculation lie above those of the experiment.

The deviations at low energies may indicate, as expected, that the model works best for heavy nuclides. It is, however, noted that the cross-section data at 160 MeV indicate that the model works quite well for light elements. The deviations at 10 deg for high energies may result from a failure of the calculation to faithfully predict the small-angle neutron production. To summarize, the cross-section calculations are in good agreement with experiment; however, the thick-target comparisons suggest that more study is required at low energies and at small angles.

ACKNOWLEDGMENTS

The authors wish to thank Harvard University and the Office of Naval Research, Department of the Navy, for use of the synchrocyclotron and, in particular, A. Koehler of the Harvard University Physics Department for his aid and advice during the experiment. The aid of C. F. Johnson of General Dynamics, Fort Worth, Texas, in the design and performance of the experiments is gratefully acknowledged. Thanks are also due to W. E. Kinney of the Oak Ridge National Laboratory for writing the Monte Carlo codes for calculating the efficiency and resolution of the spectrometer and to R. T. Santoro for assistance in beam calibration. The contribution of N. W. Hill in designing much of the electronics and aiding in the execution of the experiment is greatly appreciated.